Localization of Pom121 to the inner nuclear membrane is required for an early step of interphase nuclear pore complex assembly

Tomoko Funakoshi[a,b], Michaela Clever[a], Ai Watanabe[a], and Naoko Imamoto[a]
[a]Cellular Dynamics Laboratory and [b]Live-Cell Molecular Imaging Research Team, Riken Advanced Science Institute, Saitama 351–0198, Japan

ABSTRACT The nuclear pore complex (NPC) is a large protein assembly that mediates molecular trafficking between the cytoplasm and the nucleus. NPCs assemble twice during the cell cycle in metazoans: postmitosis and during interphase. In this study, using small interfering RNA (siRNA) in conjunction with a cell fusion–based NPC assembly assay, we demonstrated that pore membrane protein (Pom)121, a vertebrate-specific integral membrane nucleoporin, is indispensable for an early step in interphase NPC assembly. Functional domain analysis of Pom121 showed that its nuclear localization signals, which bind to importin β via importin α and likely function with RanGTP, play an essential role in targeting Pom121 to the interphase NPC. Furthermore, a region of Pom121 that interacts with the inner nuclear membrane (INM) and lamin B receptor was found to be crucial for its NPC targeting. Based on these findings and on evidence that Pom121 localizes at the INM in the absence of a complete NPC structure, we propose that the nuclear migration of Pom121 and its subsequent interaction with INM proteins are required to initiate interphase NPC assembly. Our data also suggest, for the first time, the importance of the INM as a seeding site for "prepores" during interphase NPC assembly.

Monitoring Editor
Karsten Weis
University of California, Berkeley

Received: Jul 28, 2010
Revised: Jan 3, 2011
Accepted: Jan 19, 2011

INTRODUCTION

The eukaryotic genome is segregated from the cytoplasm by a pair of lipid bilayers referred to as the nuclear envelope (NE). The NE consists of the outer nuclear membrane (ONM), the inner nuclear membrane (INM), and nuclear pore complexes (NPCs) that span both membranes. The ONM is continuous with the endoplasmic reticulum (ER) and shows ER-like properties such as the presence of bound ribosomes. In contrast, the INM contains a distinct set of integral membrane proteins, which, in vertebrates, are connected to the nuclear lamina (Daigle *et al.*, 2001; Rabut *et al.*, 2004a; Wilson and Berk, 2010). Interestingly, the nuclear lamina provides a framework for nuclear organization as well as NPC distribution (Maeshima *et al.*, 2006), indicating that the INM provides a physical connection between the NPC and intranuclear structures.

NPCs are the sole route for molecular trafficking between the nucleus and the cytoplasm. The NPC comprises multiple copies of ~30 different proteins, termed nucleoporins (Nups), and undergoes assembly and disassembly during the cell cycle (Maul *et al.*, 1971; Rout and Aitchison, 2000; Cronshaw *et al.*, 2002; Maeshima *et al.*, 2006; Alber *et al.*, 2007). In vertebrates, NPCs assemble twice during the cell cycle: at the end of mitosis, when the NE reforms around the daughter chromosomes, and during the cell cycle on the assembled NE. The latter process is considered to be more evolutionarily conserved because in eukaryotes such as yeast that undergo closed mitosis, new NPCs assemble only on continuous double-lipid NE bilayers (Rexach, 2009). This process is essential to prepare for the next round of cell division. The underlying molecular mechanisms involved remain largely unknown, however.

This article was published online ahead of print in MBoC in Press (http://www.molbiolcell.org/cgi/doi/10.1091/mbc.E10-07-0641) on February 2, 2011.

Address correspondence to: Naoko Imamoto (nimamoto@riken.jp).

Abbreviations used: BHK, baby hamster kidney; EGFP, enhanced green fluorescent protein; ER, endoplasmic reticulum; FG, phenylalanine-glycine; FRAP, fluorescence recovery after photobleaching; GFP, green fluorescent protein; GST, glutathione *S*-transferase; GTP, guanosine-5′-triphosphate; H2B, histone 2B; INM, inner nuclear membrane; LBR, lamin B receptor; mAb, monoclonal antibody; NE, nuclear envelope; NGS, normal goat serum; NLS, nuclear localization signal; NPC, nuclear pore complex; Nup, nucleoporin; ONM, outer nuclear membrane; PBS, phosphate-buffered saline; PEG, polyethylene glycol; Pom, pore membrane protein; RCC1, regulator of chromosome condensation 1; RNAi, RNA interference; SECFP, super enhanced cyan fluorescent protein; siRNA, small interfering RNA.

It has been argued for some time whether assembly of the interphase NPC occurs by duplication and subsequent separation of existing NPCs or by a de novo process (Rabut *et al.*, 2004b). In vitro assays with *Xenopus* egg extracts and high-resolution imaging showed that new NPCs assemble on the NE by a de novo mechanism in which the scaffold Nup107–160 complex is inserted into NPC assembly sites from both the cytoplasmic and nucleoplasmic sides of the NE (D'Angelo *et al.*, 2006). Recent studies in budding yeast showed that the Nup170p complex, together with transmembrane Nups, plays an initiating role in the formation of new NPCs (Flemming *et al.*, 2009; Makio *et al.*, 2009; Onischenko *et al.*, 2009). The Nup170p complex contains "lipophilic" Nups that bind directly to membrane lipids, thus contributing to curvature of the membrane at NE sites where NPCs are to be inserted. The proposed models suggest the necessity of membrane fusion for NPC formation, a prerequisite for a de novo mechanism.

In vertebrates, three transmembrane Nups exist: pore membrane protein (Pom)121, Ndc1, and gp210. Of these, Pom121 is unique to vertebrates, whereas Ndc1 is conserved among metazoans and yeast. Pom121 comprises a short peptide domain of ~30 amino acids that inserts into the ER lumen, a single transmembrane domain, and a long (>1000-amino-acid) polypeptide domain that extends into the cytoplasm (Hallberg *et al.*, 1993; Funakoshi *et al.*, 2007).

In some, but not all, cases, Pom121 has been reported to be necessary for assembly of the postmitotic NPC (Antonin *et al.*, 2005; Mansfeld *et al.*, 2006; Stavru *et al.*, 2006; Funakoshi *et al.*, 2007). Quantitative time-lapse analysis showed that postmitotic NPC assembly, which occurs soon after the onset of anaphase, involves the recruitment of Nups to sister chromatids in an ordered, stepwise manner (Dultz *et al.*, 2008). Pom121 is one of the early Nups to be recruited to sister chromatids during postmitotic NPC assembly. In vitro assays using *Xenopus* egg extracts have revealed the molecular basis of this recruitment: Pom121 is retained in the same membrane vesicles as Ndc1 and interacts directly with components of the Nup107–160 complex and the Nup205–93 complex (the vertebrate homologue of the yeast Nup170p complex) (Antonin *et al.*, 2005). Pom121 and Ndc1 are recruited together to sister chromatids, depending on the recruitment of Nup107–160 complexes. Nup107–160 complexes associate with sister chromatids through the AT-hook DNA-binding protein ELYS/Mel28 and also bind to Pom121 (Rasala *et al.*, 2008). This association initiates assembly of the postmitotic NPC and the formation of a "prepore," which occurs on the DNA (Dultz *et al.*, 2008). Following the formation of prepores, components of the Nup205-93 complex and peripheral Nups are recruited to complete postmitotic NPC formation (Dultz *et al.*, 2008).

We previously reported that the human genome encodes two different full-length Pom121 genes, which are both transcribed and translated in HeLa cells (Funakoshi *et al.*, 2007). Efficient depletion of Pom121 using small interfering RNA (siRNA) reduced the NPC number, which suggested the necessity of Pom121 for NPC assembly or the maintenance of NPC structure. Furthermore, depletion of Pom121 induced NPC clustering and the formation of aberrant nuclear structures, suggesting that the biogenesis and/or organization of NPCs somehow influence the structure and/or stability of the nucleus. These phenomena reinforce the idea that NPC structure and INM structure are linked.

In the present study, we demonstrated, using a live imaging system that we recently developed (Maeshima *et al.*, 2010), that Pom121 is required for formation of the interphase NPC. We examined how ER-translated Pom121 becomes incorporated into the NPC, an event we anticipated to be important for interphase NPC formation. We found that Pom121 contains two previously uncharacterized functional domains essential for its localization to NPCs: a region that interacts with components of the INM, including lamin B receptor (LBR), and multiple nuclear localization sequence (NLS) that bind to importin β via importin α, which are likely to function through RanGTP. The requirement for NLSs for the NPC localization of Pom121 is interphase specific because they are not essential for the targeting of Pom121 to sister chromatids during postmitotic NPC assembly. We further demonstrated that, consistent with its nuclear localization activity and INM-binding properties, Pom121 indeed localized to the INM. On the basis of these results, we propose that Pom121 is transported into the nucleus through nuclear pores by a mechanism involving Ran and importins and subsequently binds to INM proteins prior to its incorporation into the NPC. Unlike postmitotic NPC assembly, in which "prepores" are seeded on mitotic chromosomes by ELYS, our results suggest the importance of the INM as a site on which Pom121 marks loci for the seeding of "prepores" during de novo interphase NPC formation.

RESULTS

Pom121 is required for interphase NPC formation in dividing human cells

We tested whether Pom121 was necessary for interphase NPC formation through the combined application of siRNA and a cell-fusion–based method developed in our laboratory that allows the formation of NPCs on assembled NEs to be visualized (Figure 1) (Maeshima *et al.*, 2010). Cells stably expressing the yellow fluorescent protein derivative Venus fused to Nup107, a scaffold protein that is essentially immobile in NPCs, were used as donor cells, and cells stably expressing super enhanced cyan fluorescent protein (SECFP) fused to histone 2B (H2B) were used as acceptor cells. G_1-synchronized donor and acceptor cells were fused using polyethylene glycol (PEG) to generate "heterokaryons," which were then incubated for 16 h with aphidicolin, a chemical that prevents cells from entering mitosis by inhibiting DNA synthesis, but that does not interfere with interphase NPC formation. Immediately after fusion (0 h), a large number of Venus fluorescent dots were detected on donor nuclei derived from Venus-Nup107–expressing cells but not on acceptor nuclei derived from SECFP-H2B–expressing cells. At 16 h postfusion, the rims of acceptor nuclei, which display brighter SECFP–H2B signals in aphidicolin-treated heterokaryons, were covered with numerous bright Venus fluorescent dots (7.2-fold increase in fluorescence intensity compared with the time 0 intensity of siRNA untreated acceptor cell nuclei; see Figure 1Cb), representing NPCs formed during the 16-h incubation period. When acceptor cells were treated with siRNA targeted to Pom121 prior to cell fusion (which resulted in ~50% decrease in the intensity of the Pom121 signal; see Figure 1Ca and Supplemental Figure S1A), however, fewer Venus-Nup107 fluorescent dots were detected on acceptor nuclei, even after 16 h (35% decrease in intensity of Venus-Nup107 signal compared with that of nontreated nuclei [16 h]; see Figure 1Cb). This evidence that the depletion of Pom121 prevents the appearance of Nup107 signals on acceptor nuclei clearly demonstrates the indispensable role of Pom121 in NPC formation in HeLa cells during interphase.

In subsequent studies, we attempted to identify the functional domain of Pom121 required for interphase NPC assembly by determining the Pom121 elements responsible for its targeting to NPCs. The human genome contains two distinct Pom121 genes, Pom121-A and Pom121-C, both of which are transcribed and translated (Funakoshi *et al.*, 2007). Pom121-A was used to identify Pom121's functional regions. Various Pom121 deletion fragments were fused either to green fluorescent protein (GFP) derivatives or to glutathione

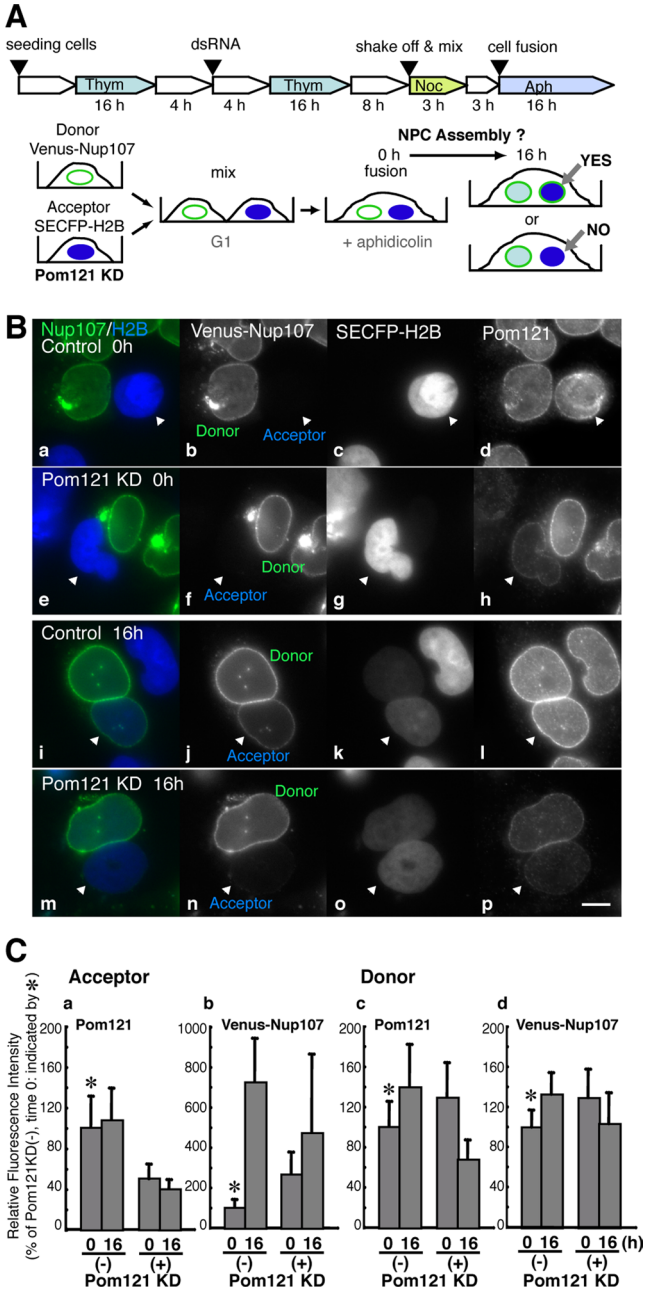

FIGURE 1: Pom121 is required for interphase NPC assembly. (A) Schematic representation of the interphase NPC assembly assay. Cells stably expressing Venus-Nup107 were used as donors, and others stably expressing SECFP-H2B as acceptors. Between thymidine treatments, acceptor cells were transfected with double-stranded RNA (dsRNA) targeted to Pom121. G_1-synchronized donor and acceptor cells were treated with PEG to generate heterokaryons. (B) Effect of Pom121 knockdown (KD) on interphase NPC assembly. Immediately after fusion (0 h, a–h), donor nuclei derived from Venus-Nup107 cells displayed bright fluorescent dots (representing NPCs), whereas no such dots were detected in the acceptor nuclei from SECFP-H2B–expressing cells (b and f). At 16 h postfusion (16 h, i–p), numerous fluorescent dots were observed on the acceptor nuclei of aphidicolin-treated heterokaryons (j). In contrast, very few Venus-Nup107 dots were observed in heterokaryons fused with Pom121 KD acceptor cells, even at 16 h after fusion (n). Arrowheads indicate acceptor nuclei in heterokaryons. Scale bar, 10 μm. (C) Quantification results of fluorescence intensities of Pom121 and Venus-Nup107 at the nuclear rim of nuclei in heterokaryons. Fluorescence intensities of Venus-Nup107 (graphs b and d) or Pom121 detected by immunostaining (graphs a and c), at the rim of nuclei derived from acceptor (graphs a and b) and donor (c and d) cells with [KD(+)] or without [KD(–)] Pom121 RNAi treatment were measured, and mean values were plotted. Standard deviations were shown as relative percentages of the level of the Pom121 KD(–) at time = 0 (marked with asterisks in graphs). Pom121KD(–): n = 4 (0 h), n = 22 (16 h). Pom121KD(+): n = 9 (0 h), n = 32 (16 h). In acceptor cell nuclei, Pom121 RNAi treatment reduced the Pom121 to ~50% of nontreated control nuclei: Compare time 0 of Pom121KD (–) and Pom121KD (+) in graph a. In Pom121 RNAi nontreated cells, which did not prevent the NPC assembly during interphase, the mean Venus-Nup107 fluorescence intensity signals of the acceptor nuclei had increased 7.2-fold during the 16-h incubation in heterokaryons: Compare 0 h and 16 h of Pom121 KD (–) in graph b. In Pom121 KD cells, the mean Venus-Nup107 signal intensity of acceptor nuclei was reduced to 65% of RNAi nontreated cell level at 16 h postfusion: Compare 16 h of Pom121 KD (–) and Pom121 KD (+) in graph b.

S-transferase (GST). The nomenclature used to describe the constructs used in this study is indicated by the Pom121-A amino acid residues present in each deletion fragment.

Pom121 contains multiple NLSs required for its localization to NPCs during interphase

We previously reported that the N-terminal region of human Pom121, which includes the transmembrane domain, was missing from all cDNAs registered in public databases (Funakoshi *et al.*, 2007). The protein encoded by truncated Pom121 cDNAs ($Pom121^{266–1249}$) is not targeted to the NE but instead migrates into the nucleus (despite its molecular weight's being above the size limit for passive diffusion across the NPC permeability barrier), whereas full-length Pom121 ($Pom121^{1–1249}$) is specifically targeted to the NPC (Funakoshi *et al.*, 2007) (Figure 2, C and Da). This previous finding indicates that human Pom121 must possess one or more NLSs, although their biological significance is not yet clear.

We next attempted to identify Pom121's NLSs. To this end, we constructed a series of deletion mutants and expressed them as enhanced green fluorescent protein (EGFP) fusion proteins to examine their subcellular localization. This analysis revealed that the sequences responsible for the nuclear import of Pom121 were exclusively contained within $Pom121^{266–702}$ (Figure 2, A and C, and Supplemental Figures S2 and S3), as an N-terminal Pom121 fragment containing the transmembrane region ($Pom121^{1–265}$) only diffusely localized to the ER and NE (Figure 3Bc and Supplemental Figure S3b), similar to rat Pom121 (Söderqvist *et al.*, 1997), whereas a C-terminal fragment containing the phenylalanine-glycine (FG) repeats ($Pom121^{703–1230}$) displayed no or weak nuclear localization activity (Supplemental Figure S2Ba).

We identified putative NLSs in $Pom121^{266–702}$ based on the presence of clusters of basic amino acid residues, which are conserved between human and rat Pom121. To examine their nuclear localization activities, the fragments containing these putative NLSs were cloned and expressed. If the observed nuclear localization activity was abrogated through the substitution of basic amino acids with alanine (Ala), we assigned the sequence as an NLS (Supplemental Figure S2). As a result, five basic clusters were identified as NLSs. Their positions and sequences are shown in Figure 2B (see also Supplemental Figure S1B).

As shown in Figure 2Cd, when five Ala mutations were introduced into $Pom121^{266–1249}$ ($Pom121^{266–1249}$NLSmut), its nuclear localization was lost, suggesting that no further NLSs existed in this region. When the same five Ala mutations were introduced into

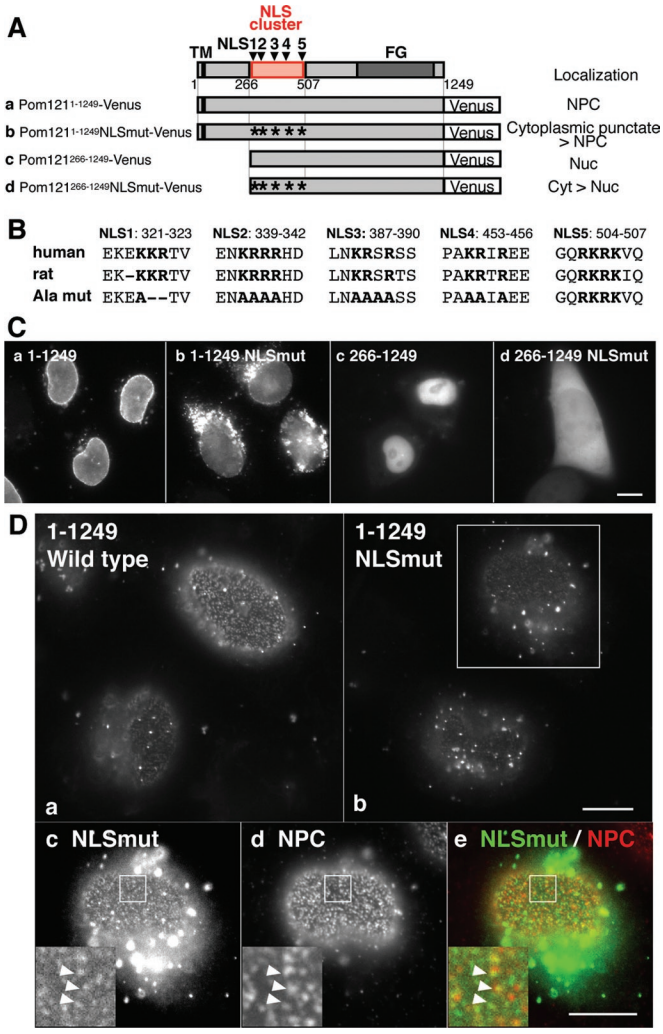

FIGURE 2: Multiple NLSs are required for the targeting of Pom121 to NPCs. (A) Schematic representations of the Pom121 N-terminal deletion fragments, with and without NLS mutations. Arrowheads indicate the positions of the five NLSs, and asterisks indicate the basic amino acid (K or R) within each NLS that was replaced with Ala. TM, transmembrane domain; NLS cluster, NLS-containing region (amino acids 266–513); FG, FG repeat-rich region. (B) Sequences of the NLSs within human Pom121 identified in this study and the corresponding regions of rat Pom121. The positions of the alanine substitution mutations (Ala mut) are indicated. (C) Subcellular localization of (a) full-length Pom121$^{1–1249}$-Venus, (b) full-length Pom121$^{1–1249}$ carrying mutations in all five NLSs (the basic amino acids in NLS1-NLS5 were replaced with alanine residues, as indicated in B), (c) an N-terminally truncated deletion mutant Pom121$^{266–1249}$, and (d) an N-terminally truncated deletion mutant carrying mutations in all five NLSs Pom121$^{266–1249}$ NLSmut (following their transient expression in HeLa cells). (D) Visualization at higher intensity and magnification revealed the localization of Pom121$^{1–1249}$NLSmut-Venus at NPCs (stained with mAb414). Top panels: HeLa cells transiently expressing wild-type Pom121 (a) or Pom121 NLSmut-Venus (b). Bottom panels: enhanced and enlarged versions of the inset images in panel b (NLSmut). c: Pom121$^{1–1249}$NLSmut-Venus; d: NPCs stained with mAb414; e: merged image. Colocalization of the Pom121$^{1–1249}$NLSmut-Venus and mAb414 signals is indicated by arrowheads. Bar, 10 μm.

full-length Pom121$^{1–1249}$ (Pom121$^{1–1249}$NLSmut), most of the mutant protein localized to cytoplasm, which was detected as punctate dots, instead of NPC (Figure 2Cb). This finding illustrates the importance of NLSs for the targeting of Pom121 to NPCs during interphase. It must be noted, however, that when photos were taken with longer exposure times, we could observe Pom121$^{1–1249}$NLSmut co-localizing with NPC visualized by monoclonal antibody (mAb)414 staining, although the colocalization was partial (Figure 2D, b–e) because Pom121$^{1–1249}$NLSmut can become incorporated into the NPC during postmitotic NPC assembly (see Figure 5 later in this article).

The minimum region of Pom121 containing all elements required for its targeting into NPCs during interphase

We next attempted to better define the elements required for Pom121 to target the NPCs during interphase. An N-terminal fragment containing the transmembrane domain (amino acids 35–55, predicted), Pom121$^{1–265}$ localized to the ER and NE but not to NPCs (Figure 3Bc and Supplemental Figure S3b). When the Pom121$^{266–494}$ fragment, which possessed strong nuclear import activity (Supplemental Figure S3c), was combined with this Pom121$^{1–265}$ fragment, the resulting Pom121$^{1–494}$ not only localized to the nuclear rim, but, like full-length Pom121, specifically colocalized with NPCs, as shown by mAb414 staining (Figure 3Bb; compare also Supplemental Figure S3, a and b). This finding indicates that the C-terminal portion of Pom121, which contains long stretches of FG repeats, does not play a prominent role in its NPC localization, and reinforces the importance of the N-terminal portion, Pom121$^{1–494}$, for its targeting to the NPC during interphase.

Our analysis presented in Figure 2B shows that Pom121$^{1–494}$ contains four NLSs (NLS1–NLS4) within the region comprising amino acids 266–494. When Ala mutations were introduced into all the four NLSs, the resulting mutant protein, Pom121$^{1–494}$NLSmut, dispersed diffusely throughout the ER, as anticipated (Figure 3Bf and Supplemental Figure S3e). When an SV40 T-antigen NLS was conjugated to the C terminus of Pom121$^{1–494}$NLSmut, which lacks NPC targeting activity, the resulting protein, Pom121$^{1–494}$NLSmut+T-NLS, was targeted to NPCs (Figure 3Bg and Supplemental Figure S3f). These findings reinforce the importance of NLS activity for the targeting of Pom121$^{1–494}$ to the NPC. Notably, conjugation of the SV40 T-antigen NLS to Pom121$^{1–265}$ targeted this Pom121 fragment to the nuclear rim, but not to the NPC (Figure 3Bd), indicating that amino acids 266–494 of Pom121 contain additional elements besides the identified NLSs that are required for targeting Pom121 to NPCs.

We identified Pom121$^{1–494}$ as the minimum region containing all the elements required for Pom121 to target to the NPC during interphase (see later in the text).

Pom121contains an NE-binding region involved in NPC targeting

When the first 136 amino acids, including those that make up the transmembrane domain, were deleted from the N terminus of Pom121$^{1–494}$ (Pom121$^{137–494}$), the resulting fragment localized to the NE (Supplemental Figure S3d). Interestingly, however, imaging of the nuclear surface under higher magnification showed that it did not colocalize with the NPCs (Figure 3Be), indicating the importance of Pom121's transmembrane region (amino acids 1–136) for the targeting of Pom121$^{1–494}$ to NPCs, in agreement with a previous report (Söderqvist *et al.*, 1997). When the same N-terminal portion was deleted from full-length Pom121, the resulting fragment, Pom121$^{137–1249}$, localized to the NPC (Figure 4, Bd and Cd). The respective localization of Pom121$^{137–494}$ and Pom121$^{137–1249}$ to the NE and NPC may reflect redundancy in the physical retention of Pom121 at the NPC by the transmembrane domain and the C-terminal region, in the latter case, possibly by FG repeats.

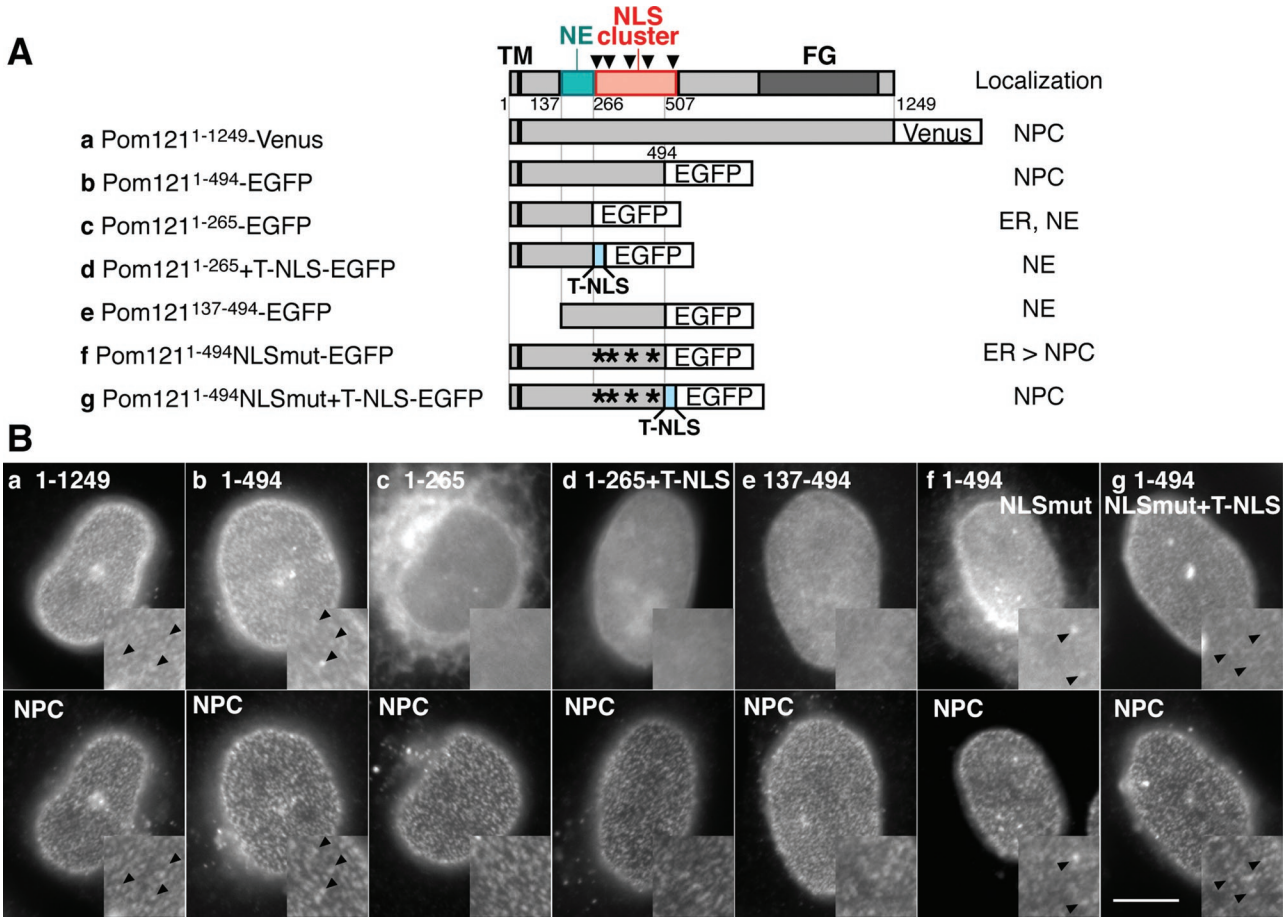

FIGURE 3: The minimum region of Pom121 required for its targeting to the NPCs. (A) Schematic representation of the Pom121 N-terminal fragments. Arrowheads and asterisks indicate the positions of the five NLSs and the Ala substitution mutation in each NLS, respectively. The subcellular localizations of transiently expressed Pom121 fragments indicated to the right are based on the observations described in Figure 3B and Supplemental Figure S3. T-NLS, SV40 large T antigen NLS; NE, inner NE-binding region; otherwise as in Figure 2A. (B) High-magnification images of the nuclear surfaces of cells transiently expressing Venus or EGFP-tagged Pom121 fragments, which were immunostained with anti-GFP antibody (top panels) and mAb414 (bottom panels). Arrowheads indicate colocalization of the Pom121 and NPC signals. Bar, 10 μm.

In contrast to Pom121$^{137–494}$ and Pom121$^{137–1249}$, mutants created through further N-terminal truncation, Pom121$^{266–494}$ and Pom121$^{266–1249}$, were not targeted to the NE, but instead entered the nucleus as described earlier in text (Figure 2Cc and Supplemental Figure S3c). We thus questioned whether the region comprising amino acids 137–265, which influenced the localization of Pom121, formed any interactions with the NE. To test this, we expressed Pom121$^{137–265}$ as an EGFP fusion and examined its subcellular localization. As shown in Figure 4Ba, Pom121$^{137–265}$ localized to the ER and NE. It did not localize to the NPC (Figure 4Ca). Comparison of Triton X-100 treatment after fixation with digitonin treatment prior to fixation showed that Pom121$^{137–265}$ attached not only to the ER, but also, like lamin B, to the INM (Supplemental Figure S4, G–I; see also Figure 7C; full-length Pom121 lacking amino acids 137–265 (Pom121$^{1–1249}$ΔNE) displays reduced INM binding). We will thus hereafter refer to this fragment as the NE-binding region.

When the NE-binding region (amino acids 137–265) was deleted from both Pom121$^{1–494}$ and full-length Pom121, the resulting mutants, Pom121$^{1–494}$ΔNE and Pom121$^{1–1249}$ΔNE, respectively, were primarily detected as small dots either attached to the nuclear rim or in the cytoplasm. Neither fragment colocalized with NPCs (Figure 4, Bb, Bc, Cb, and Cc). These results indicate that the NE-binding region of Pom121 is necessary for its targeting to NPCs.

Taken together, the results of these thorough analyses show that at least two elements of Pom121 are indispensable for its NPC targeting: the NE-binding region (amino acids 137–265) and multiple NLSs.

Roles of Pom121 NLSs and Pom121 NE-binding regions on assembly of the postmitotic NPC

We next examined whether NLSs and the NE-binding region of Pom121 are required for its targeting to sister chromosomes during postmitotic NPC assembly. To answer this question, we stably expressed full-length wild-type Pom121 (Pom121$^{1–1249}$), a mutant form of Pom121 carrying five NLS mutations (Pom121$^{1–1249}$ NLSmut), and a Pom121 mutant lacking the NE-binding region (137–265 amino acids: Pom121$^{1–1249}$ΔNE) and compared their targeting to telophase chromatids. As shown in Figure 5, both Pom121$^{1–1249}$NLSmut and Pom121$^{1–1249}$ΔNE are targeted to sister chromosomes. Closer examination of the Venus signals arising from Pom121 mutants on the surfaces of chromosomes showed that Pom121$^{1–1249}$NLSmut existed as dots that colocalized with NPCs visualized by mAb414 staining, whereas much less Pom121$^{1–1249}$ΔNE signal colocalized with NPCs. When compared with wild-type Pom121$^{1–1249}$, the Venus signal intensities colocalized with NPC on chromosome surfaces were lower for both

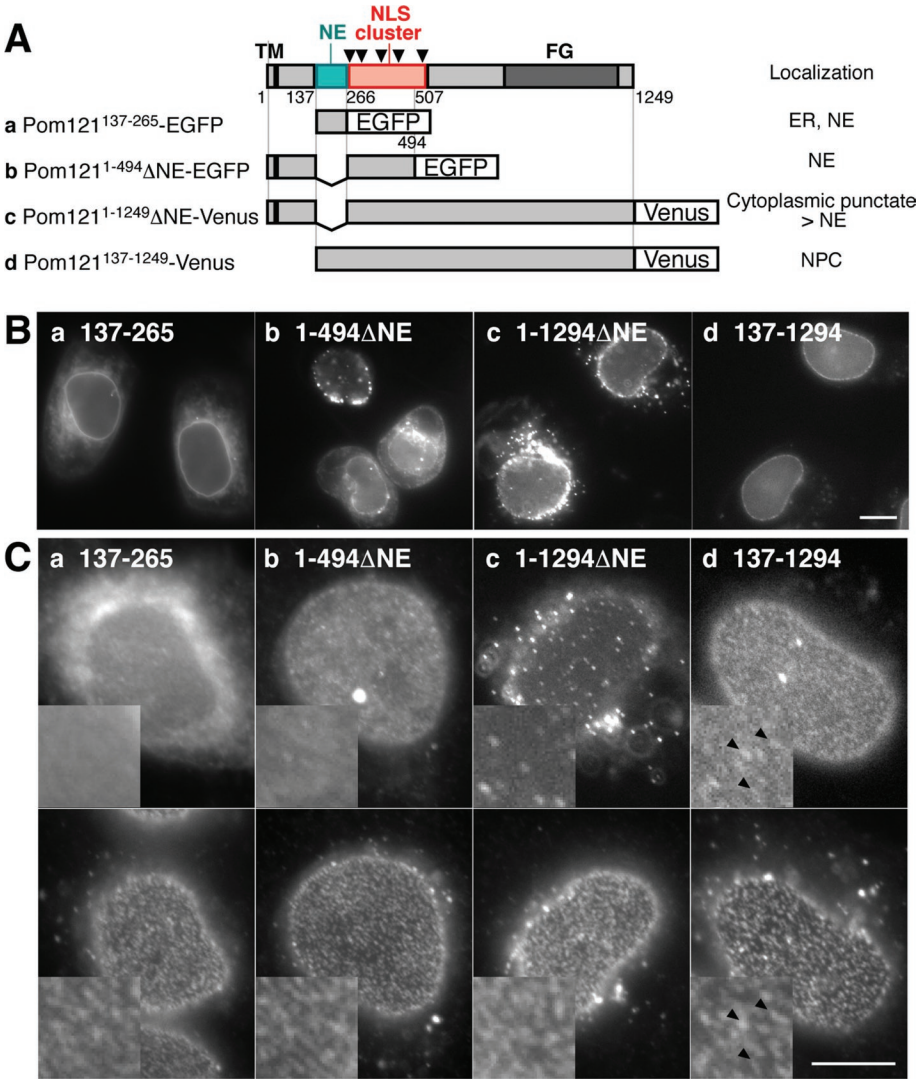

FIGURE 4: The NE-binding region is required for the targeting of Pom121 to NPCs. (A) Schematic representation of the inner NE-binding region (Pom121$^{137–265}$), the NE-binding sequence–deleted mutants from either Pom121$^{1–494}$ or full-length Pom121 (Pom121 Pom121$^{1–494}$ΔNE or Pom121$^{1–1249}$ΔNE), and the transmembrane domain deletion mutant (Pom121$^{137–1249}$). (B) Subcellular localization of transiently expressed Pom121 fragments. Middle sections showing the indicated Pom121 fragments, expressed as EGFP or Venus fusions as in A. (C) Nuclear surfaces of cells transiently transfected with Pom121 fragments as in B visualized by coimmunostaining with an anti-GFP (top panels) antibody and mAb414 (NPC, bottom panels). Arrowheads indicate the colocalization of Pom121 and NPCs. Bar, 10 μm.

mutants (see Figure 5). These results indicate that the NE-binding domain is involved in a postmitotic NPC assembly, whereas the NLSs may have less important roles. Accordingly, closer, high-intensity examination of the nuclear surfaces of cells expressing Pom121$^{1–1249}$NLSmut revealed that Pom121$^{1–1249}$NLSmut partially colocalizes with NPCs (as visualized by mAb414 staining), suggesting that it is incorporated into NPCs during postmitotic NPC assembly (Figure 2D).

Binding partners of the Pom121 functional domains

We next tested whether Pom121 interacted with members of the importin family via its NLSs. Immunoprecipitation analyses performed using an anti-GFP antibody and protein samples from cells expressing Pom121$^{1–1249}$-Venus showed that Pom121 interacted with importin β and several Nups, including Nup107, Nup53, Nup153, and ELYS (unpublished data), consistent with the results of a recent study (Rasala *et al.*, 2008). The FG repeats in Pom121's C-terminal region are not required for the targeting of Pom121 to NPCs but do bind to nuclear transport carriers, which may cause cargo proteins to be indirectly pulled down in assays. To avoid any confusion, we performed pull-down assays using GST-fused Pom121$^{266–513}$, which contains all five identified NLSs, but no FG repeats. As shown in Figure 6B, GST-Pom121$^{266–513}$ interacted with importin α and importin β in whole-cell extracts. This peptide also interacts with Nup107 and Nup53, although its interaction with Nup53 may not be strong (Figure 6D, top panels). The interactions with Nup107 and Nup53 both depend on the presence of NLSs; therefore they could be interacting through importin β binding and not directly. Pull-down assays performed using purified recombinant proteins confirmed that the interaction of GST-Pom121$^{266–513}$ with importin β was dependent on direct binding of importin α to the NLSs of the Pom121 fragment (Figure 6C).

On the basis of its localization to the INM, we next tested the ability of the NE-binding region, Pom121$^{137–265}$, to bind to specific INM components. To this end, we performed pull-down assays using GST-Pom121$^{137–513}$, which contains the NE-binding region and the region containing all five NLSs, and whole-cell extracts. GST-Pom121$^{137–513}$ interacted with ELYS, Nup153, and LBR but not with lamin B (Figure 6E). Of these binding partners, LBR formed the strongest binding interaction, which did not depend on the NLSs (Figure 6E), but was lost when the NE-binding region was deleted (Figure 6D, bottome panels). These results indicate that the NE-binding region of Pom121 interacts with LBR, an INM component.

Pom121 has affinity for the inner membrane in the absence of NPCs

Recently it was reported that a C-terminal deletion in LBR caused the two membranes comprising the NE to separate (Zwerger *et al.*, 2010). Expression of one of the tested mutants, comprising amino acids 1–533 of LBR (LBR$^{1–533}$), induced separation of the ONM and INM in U2OS cells. We took advantage of this observation to examine whether Pom121 can localize to the INM. We found that Pom121$^{1–1249}$-Venus localized to the INM in U2OS cells expressing mCherry-LBR$^{1–533}$ (Figure 7A). Immunofluorescence staining of endogenous Pom121 and RanGAP showed RanGAP, which specifically binds to a cytoplasmic component of the NPC, RanBP2, to be associated with the intact NE, but not the separated INM, showing the complete NPC structure to be absent from the disrupted NE.

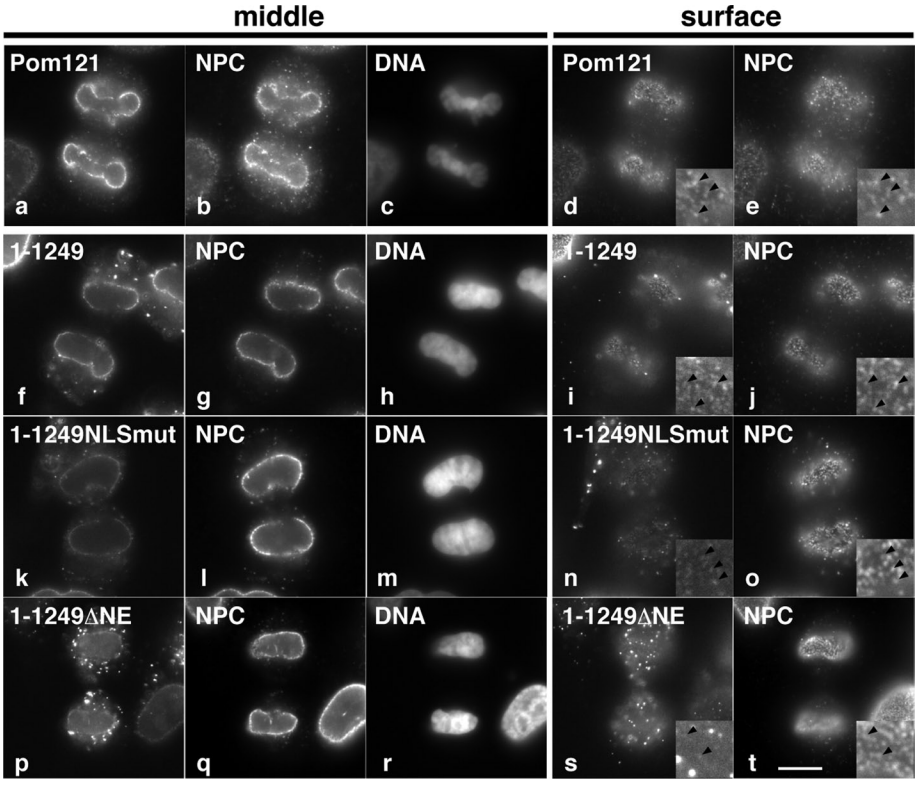

FIGURE 5: The NLSs of Pom121 are not required for postmitotic NPC assembly. Endogenous Pom121 was visualized in most top panels (a–e), whereas localization of stably transformed wild-type Pom121-Venus or its mutant proteins were visualized in the bottom panels (f–j, k–o, p–t). Images show HeLa cells stained with Pom121 (a and d) and mAb414 (b and e) antibodies [middle sections (a–c); nuclear surfaces (d and e)]. Images show HeLa cells stably expressing wild-type Pom121$^{1–1249}$-Venus [middle sections (f–h); nuclear surfaces (i and j)], the NLS mutant Pom121$^{1–1249}$NLSmut-Venus [middle sections (k–m); nuclear surfaces (n and o)], or Pom121$^{1–1249}$ΔNE [middle sections (p–r); nuclear surfaces (s and t)], costained with anti-GFP and mAb414 to visualize NPCs. Inset: enlarged images of nuclear surfaces, showing Pom121 and NPC signals. Arrows indicate the colocalization of Pom121 with NPCs. DNA; DAPI stained. Bar, 10 μm.

In contrast, endogenous Pom121 was detected at both the separated INM and the intact NE (Figure 7B), which shows that Pom121 localizes to the INM in the absence of complete NPCs. Notably, Pom121 lacking the NE-binding region (amino acids 137–265; Pom121$^{1–1249}$ΔNE) displayed significantly decreased INM localization under the same conditions, reinforcing the importance of this region for interacting with INM (Figure 7C). These results corroborate these data describing the potential of Pom121 to interact with the INM (see also Supplemental Figure S4, G–I) and the INM protein LBR (Figure 6E).

The importin-Ran system mediates the targeting of Pom121 to NPCs

It is well accepted that cellular functions mediated by importin β, including nuclear transport, require the guanosine-5′-triphosphate (GTP)-bound form of the small GTPase Ran. Given that the biochemical data described earlier in text showed that Pom121's NLS region, which is essential for its targeting to NPCs during interphase, binds to importin β through importin α, we examined whether RanGTP was required for the targeting of Pom121 to NPCs. To achieve this, we used tsBN2 (Nishimoto *et al.*, 1978), a cell line derived from baby hamster kidney (BHK) cells harboring a temperature-sensitive point mutation in regulator of chromosome condensation 1 (RCC1), a Ran guanine-nucleotide exchange factor. When tsBN2 cells are exposed to a nonpermissive temperature, RCC1 is rapidly inactivated and degraded, thus causing RanGTP levels to be depleted (Nishitani *et al.*, 1991). We transfected tsBN2 cells with Pom121$^{1–494}$, the minimum region of Pom121 necessary for its targeting to NPCs. We then determined the subcellular localization of Pom121$^{1–494}$ at permissive and nonpermissive temperatures to evaluate the contribution of RanGTP to its appropriate targeting. At a permissive temperature, RanGTP was generated, and Pom121$^{1–494}$ localized to the nuclear rim, being detected, as in HeLa cells, as punctate dots, which colocalized with NPCs visualized with mAb414 staining (Figure 8A, b, c, and d). After incubation at a nonpermissive temperature for 7 h, Pom121$^{1–494}$ was found to be mislocalized to the cytoplasm, where it formed punctate structures. A return to the permissive temperature, however, allowed Pom121$^{1–494}$ to be retargeted to the nuclear rim within 20 min (Figure 8A, e–g). Notably, many of the returned Pom121$^{1–494}$ signals are unlikely to be incorporated to NPC (visualized by mAb414 staining) within 20 min after temperature shift-down (Figure 8A, h and i). We consider that this is because of a short time of incubation after temperature shift-down, because Pom121$^{1–494}$ expressed in tsBN2 colocalizes with NPC at permissive temperatures. As shown in Figure 8B, Fluorescence recovery after photobleaching (FRAP) analysis showed Pom121$^{1–494}$ to be more mobile than full-length Pom121$^{1–1294}$, which suggests that the C-terminal portion of Pom121, possibly the FG repeats, could be contributing to the stabilization of Pom121 in NPC structures. These results reveal the importance of RanGTP for the targeting of Pom121 to NPCs, with RanGTP likely functioning in concert with the importin system.

DISCUSSION

In this study, we demonstrated, using the cell fusion–based method, the importance of Pom121 for interphase NPC assembly. Pom121's INM binding and nuclear import activities, which are critical for the proper targeting of Pom121 to the interphase NPC, are likely to play important roles in interphase NPC assembly, as outlined in the model depicted in Figure 8C.

Pom121 is required for interphase NPC formation

Using cell fusion–based methods, we demonstrated that Pom121 is required for interphase NPC assembly (Figure 1). We previously reported that efficient knockdown of Pom121 reduces NPC signals (detected using mAb414), indicating that it is also required for postmitotic NPC assembly (Funakoshi *et al.*, 2007). Thus, in the experiments described in Figure 1, we used only Pom121 RNA interference (RNAi)-treated acceptor cells in which the expression level of endogenous Pom121 was only reduced to ~50% of that in siRNA-nontreated cells [based on fluorescence intensities (Figure 1Ca) and the results of Western blotting (Supplemental Figure S1A)]. Under

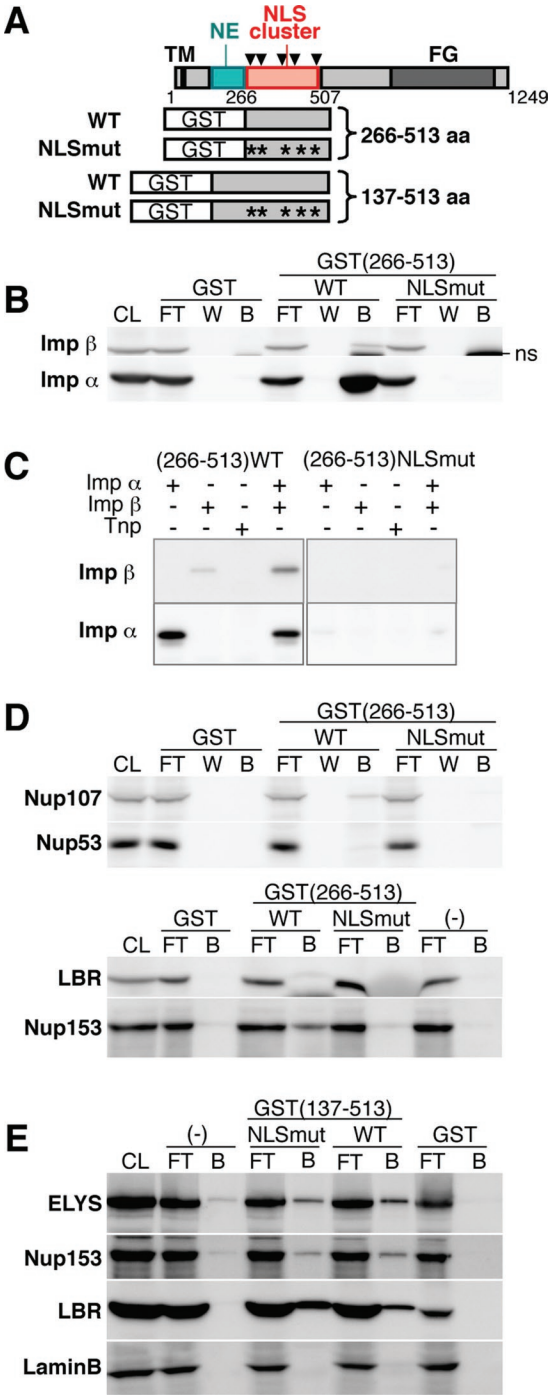

FIGURE 6: Binding partners of the Pom121 functional domains. (A) Schematic representation of the GST-Pom121 fragments used in pull-down assays. Arrowheads and asterisks indicate the positions of the five NLSs and the Ala substitution mutation in each NLS, respectively. (B) Pull-down analysis performed using GST-Pom121$^{266–513}$ and the NLS mutant GST-Pom121$^{266–513}$NLSmut. CL, cell lysate (input); FT, flow through (unbound); W, last wash; B, bound fraction; ns, nonspecific band. Comparison of the wild-type (WT) and mutant (NLSmut) lanes indicates that Pom121$^{266–513}$ interacts with importin α and β via its NLSs. (C) Pom121 NLSs binds to importin β via importin α. Purified GST-Pom121$^{266–513}$ fragments were incubated with recombinant proteins (see *Materials and Methods*). Bound proteins were separated by SDS–PAGE and detected by Western blotting. Imp α, importin α; Imp β, importin β; Tnp, transportin. Pom121$^{266–513}$ interacts with importin β via direct interactions between its NLSs and importin α. (D and E) The INM protein LBR interacts with Pom121. GST-Pom121$^{266–513}$ (NLS cluster; D) and GST-Pom121$^{137–513}$ (NE-binding region and NLS cluster; E) were used in pull-down assays. GST or beads without protein (–) were used as controls. Interactions between Nup107, Nup53, and Nup153 with Pom121$^{266–513}$ were decreased by NLS mutations. Pom121$^{137–513}$ bound to LBR, as well as ELYS and Nup153, in the absence of functional NLSs.

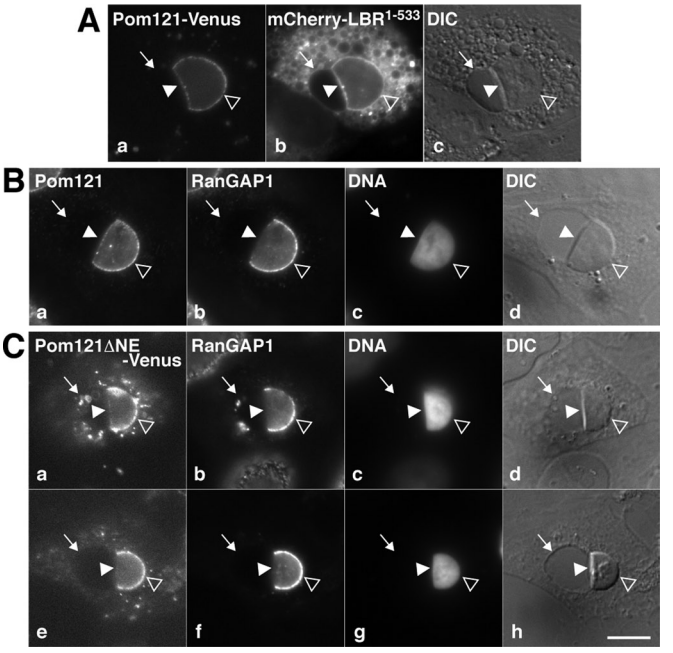

FIGURE 7: Pom121 localizes to the INM. (A) Live imaging of full-length Pom121$^{1–1249}$-Venus, transiently expressed in U2OS cells. Images were captured 14 h postcotransfection with Pom121-Venus and mCherry-LBR$^{1–533}$. (B) His-tagged LBR$^{1–533}$ was transfected into U2OS cells, and 14 h after transfection cells were fixed, immunostained with antibodies raised against Pom121 and RanGAP1, and counterstained with DAPI. (C) Venus-tagged Pom121$^{1–1249}$ΔNE and mCherry-LBR$^{1–533}$ (unpublished data) were cotransfected into U2OS cells, which were then immunostained with an antibody raised against RanGAP1 and counterstained with DAPI (as in B). Note the separation of the INM (arrowhead) and ONM (arrow). Pom121$^{1–1249}$-Venus and endogenous Pom121 were both detected at the intact NE (open arrowhead) and the separated INM (arrowhead), whereas RanGAP was detected only at the intact NE. Pom121$^{1–1249}$ΔNE-Venus localized to the INM, but at reduced levels. Bar, 10 μm.

these conditions, postmitotic NPC assembly was not strongly inhibited, at least in the observed cells, because we observed the growth of Pom121 RNAi-treated acceptor-cell nuclei during a 16-h incubation period in heterokaryons, which support the presence of nuclear transport, and therefore NPCs assembled postmitosis. It should be noted that Pom121 signals in donor cell nuclei in the same heterokaryons also became weaker during this 16-h incubation period (Pom121 signal intensity at 16 h being 52% of that at time 0; see Figure 1Cc, left two graphs). We presume that the decrease of Pom121 signal in donor nuclei was because the effects of the RNAi persisted in the heterokaryons. Accordingly, the fluorescence intensity of Venus-Nup107 in the donor cell nuclei in these heterokaryons was only ~78% of that in control cells at 16 h (see Figure 1Cd). These pieces of evidence again show that the reduction of Pom121 expression levels clearly correlates with the formation of new NPCs.

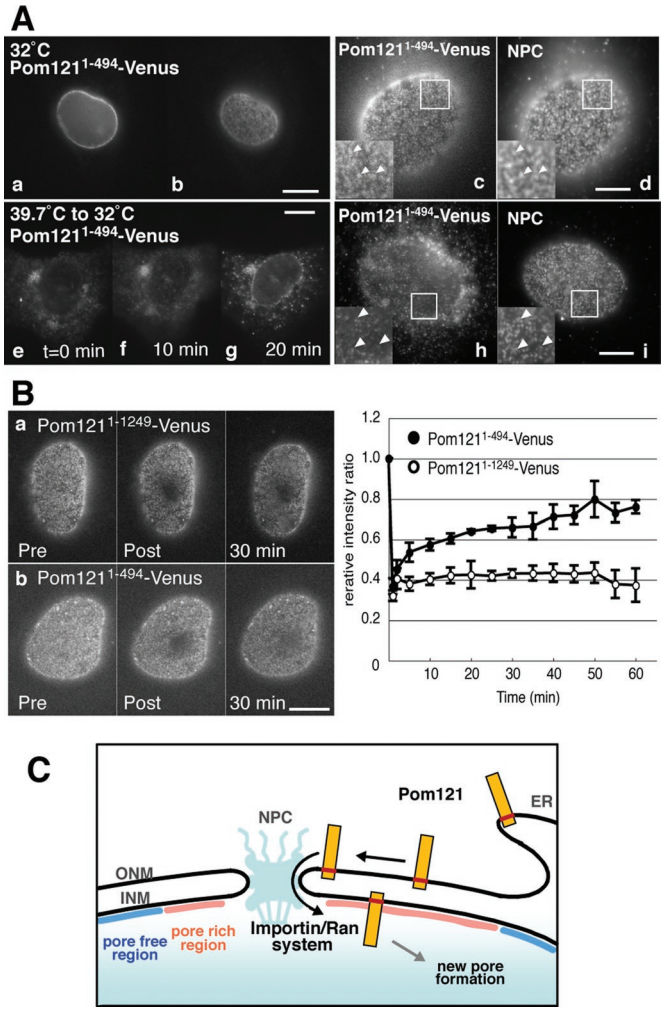

FIGURE 8: Pom121 localizes to the nuclear rim in a Ran-dependent manner. (A) a and b: Localization of transiently expressed Pom121$^{1–494}$-EGFP in tsBN2 cells cultured at a permissive temperature (32°C) after 17-h transfection. Live images of EGFP signals detected at middle sections of nucleus (a) and the nuclear surface (b) are shown. Bar,10 μm. c and d: Pom121$^{1–494}$-EGFP expressing teBN2 cells were fixed and immunostained with mAb414 antibody. Nuclear surfaces of Pom121$^{1–494}$-EGFP (c) and NPC visualized by mAb414 staining (d) are shown. Arrowheads in the high-magnification images of inlets show colocalized Pom121$^{1–494}$-EGFP and mAb414 signals. Bar, 5 μm. e–g: Pom121$^{1–494}$-EGFP mislocalized to the cytoplasm after incubation of cells at a nonpermissive temperature (39.7°C) for 7 h (e), but relocalized to the nuclear rim after their return to the permissive temperature (32°C) (f and g). h and i: tsBN2 cells expressing Pom121$^{1–494}$-EGFP were stained with mAb414 (NPC) 20 min after their return to the permissive temperature. Arrowheads in the high-magnification images of inlets show that Pom121$^{1–494}$-EGFP and mAb414 signals do not colocalize. Bar, 5 μm. (B) FRAP analysis of Pom121$^{1–494}$-Venus and Pom121$^{1–1294}$-Venus at NE. The intensity of a bleached NE region (1), a nonbleached NE region (2), and an area outside of the cell (3) were measured over time. Mean values with each standard deviation were plotted (n = 3). (C) Model showing the role of Pom121 and the potential route it takes to reach the INM. Pom121 synthesized in the ER as an integral membrane protein is translocated to the NE. It passes through the NPC as a membrane-anchored protein in an importin- and Ran-dependent manner and reaches INM, where it interacts with other Nups and/or INM proteins prior to the formation of new NPCs that takes place on the assembled NE.

Pom121's NLSs have active roles in its targeting to NPCs during interphase

We identified five basic NLSs in Pom121 (Figure 2B) that bind to importin β via importin α (Figure 6, B and C). Two NLS clusters of the five identified nlss have been described parallel to this study by two other groups (Doucet *et al.*, 2010; Yavuz *et al.*, 2010). Introducing Ala mutations in these NLSs abolished their ability to bind transport receptors (Figure 6, B and C) and impaired the targeting of Pom121 to the NPC during interphase (Figure 2Cb) but had less effect on NPC targeting during the postmitotic NPC assembly (Figure 5). This finding indicates that the Pom121 NLS mutant retains its protein structure, allowing it to become a component of NPCs despite its not being able to bind importins, which are known to function as chaperones. Therefore, Pom121's NLSs must have active and specific roles only in targeting Pom121 to NPCs during interphase.

The importance of the identified NLSs was further confirmed by experiments using Pom121$^{1–494}$, a fragment containing the minimum elements required for Pom121's targeting to NPCs during interphase. The localization of Pom121$^{1–494}$ to NPCs was entirely dependent on its NLSs: Pom121$^{1–494}$NLSmut, a mutant carrying NLS mutations, was not targeted to NPCs during interphase. Interestingly, however, addition of the SV40 T-antigen NLS to the C terminus of Pom121$^{1–494}$NLSmut restored its targeting to NPCs, reinforcing the conclusion that the NLSs play an active role in this process (Figure 3, Bf and Bg and Supplemental Figure S3, e and f).

In a further experiment performed using temperature-sensitive tsBN2 cells, which harbor a point mutation in RCC1, we showed that the localization of Pom121$^{1–494}$ to NPCs was dependent on RanGTP. Since importins always release their cargoes when bound to RanGTP (Vasu and Forbes, 2001; Hetzer *et al.*, 2002; Harel *et al.*, 2003a; Tahara *et al.*, 2008), the release of Pom121 from importin β must be a crucial step for both its NPC targeting and interphase NPC assembly. The requirement for RanGTP in this step agrees with several reports showing the importance of RanGTP in interphase NPC assembly (Ryan *et al.*, 2003; D'Angelo *et al.*, 2006; Iino *et al.*, 2010; Maeshima *et al.*, 2010). Because our present data demonstrate the importance of interactions between Pom121 and the INM for interphase NPC assembly (Figures 6, 4Bc, and 4Cc), we predict that Pom121 molecules enter the nucleus through the nuclear pores as an integral membrane protein bound to importin α/β. RanGTP then frees them from the importins, allowing them to interact with the INM protein LBR and other proteins critical for NPC assembly.

Important role of Pom121's NLSs in its nuclear import

The different requirements for the NLSs of Pom121 during the assembly of interphase and postmitotic NPCs must stem from assembled double-lipid NE bilayers' being present during interphase but not immediately following mitosis. A key mechanistic difference between the assembly of postmitotic and interphase NPCs is that the former involves the seeding of NPC precursors ("prepores") on mitotic chromosomes, whereas the latter is characterized by the seeding of "prepore" components on assembled NEs. We assume that Pom121 contributes to the seeding of "prepores" on the NE, possibly by "marking" the seeding sites. For Pom121 to mark the seeding site to be possible, membrane-anchored Pom121, which is translated at the ER, would need to be targeted to the NE, a process that would depend on the Pom121 NLSs that bind to importin β via importin α regulated by RanGTP. The ability of Pom121 to interact with (Figure 6E and Supplemental Figure S4) and localize to the INM (Figure 7) in the absence of NPCs further supports this notion. The NE-binding region of Pom121 is likely to play a role in its localization to the INM, and also in postmitotic NPC assembly (Figure 5). The

requirement of Pom121's NLSs and INM-binding activity for its targeting to NPCs and INM during interphase agrees well with the idea that the nuclear import of membrane-anchored Pom121, which allows it to make contact with the inner surface of the NE, is a crucial step in interphase NPC assembly.

It is generally accepted that NPCs provide the sole pathway for molecular exchange between the cytoplasm and the nucleus. Thus, the only route by which Pom121 may enter the nucleus is via NPCs. Our data suggest that the nuclear import of Pom121 is mediated by importin α/β and the small GTPase Ran. We propose a model in which the localization of Pom121 to the INM is an important step in the assembly of the interphase NPC. Like other INM proteins, Pom121 traverses the periphery of the NPC in the plane of the membrane at the edge of the nuclear pore (Figure 8C). Pom121 would have to overcome the proposed translocation size limit of ~75 kDa (Lusk *et al.*, 2007), which its cytoplasmic extension on its own greatly exceeds. No identified INM protein, however, shares Pom121's large FG repeat region. It is conceivable that this FG repeat region enables Pom121 to pass through the FG filament core of the NPC (Frey and Görlich, 2007) using importin α/β in a way that is distinct from that of other INM proteins, while remaining an integral membrane protein.

Relationship between NPCs and the INM

Our group previously reported that NPC localization is tightly linked to the nuclear lamina, a meshwork structure located underneath the NE, and proposed the existence of an NE subdomain that periodically appears and disappears during the cell cycle in dividing human cells (Maeshima *et al.*, 2006). NE subdomains enriched with NPCs (pore-rich regions) colocalize with lamin B and LBR, whereas those that do not contain NPCs (pore-free regions) are enriched with lamin A and its binding partner, emerin. More recently we found that cyclin-dependent kinases, which initiate interphase NPC assembly, also regulate the distribution of both NPCs and lamin B/LBR, but not that of lamin A (Maeshima *et al.*, 2010). These phenomena are also consistent with the notion that lamin B (and/or its binding partners, including LBR) is physically connected to NPCs, and such a connection may contribute to the recruitment of NPC components to the NE during the initiation of interphase NPC assembly.

Previously reported biochemical data, such as those demonstrating the interaction of Nup53 (Nup205 complex) with lamin B (Hawryluk-Gara *et al.*, 2005), concur with our morphological evidence of interactions between NPC and INM components such as B-type lamins and their binding partners. In this study, we provide further biochemical evidence of such interactions by showing that Pom121 binds to LBR (Figure 6E). In de novo NPC assembly, the transmembrane Nups have been considered to be candidate markers of NPC assembly sites onto which "prepores" can be seeded. If Pom121 is such a candidate, as the results of the present study suggest, its interaction with the INM could play a role in "marking" NPC assembly sites, in conjunction with other Nups that are rapidly recruited to the NE upon initiation of interphase NPC assembly. Interestingly, during submission of our manuscript, Fichtman *et al.* reported that Pom121 colocalized with the Nup107–160 complex on the inner, but not the outer, nuclear membrane in an early NPC assembly intermediate manipulated in *Xenopus* egg extract (Fichtman *et al.*, 2010). The interaction between Pom121 and the INM demonstrated in these studies may also explain a phenomenon we noted in a previous study, namely that the depletion of Pom121 strongly induces the formation of aberrant nuclear structures (see the Supplementary Movie in Funakoshi *et al.*, 2007). The depletion of Pom121 may cause defects in certain INM proteins, including those that make up the nuclear lamina. This, in turn, may disrupt the nuclear architecture.

MATERIALS AND METHODS

Cells and transfection

HeLa and U2OS cells were maintained in DMEM (12699–013; Invitrogen, Carlsbad, CA) supplemented with 10% fetal bovine serum (SH30070; Thermo Scientific, Waltham, MA) in 5% CO_2 at 37°C. tsBN2 cells (Nishimoto *et al.*, 1978) derived from BHK cells and carrying a temperature-sensitive RCC1 allele, were maintained as described earlier in text, but at 32°C, and, for RCC1 depletion, incubated at a nonpermissive temperature (39°C). For immunofluorescence and live imaging, cells were plated onto coverslips (C012001; Matsunami Glass, Osaka Japan) coated with poly-L-lysine (P1524; Sigma Aldrich, St. Louis, MO) and glass-bottom dishes (3910–035; Iwaki, Japan), respectively. Cell transfection was performed using Effectene reagent (301425; Qiagen, Valencia, CA) according to the manufacturer's instructions. Apart from those that were stably transfected, cells were assessed by live imaging analysis for localization of fluorescent protein-fused Pom121 or its deletion mutants ~20 h posttransfection or were fixed for immunofluorescence staining. To induce separation of the INM and ONM, an LBR deletion mutant containing amino acids 1–533 was expressed in U2OS cells (Zwerger *et al.*, 2010) as an N-terminal fusion with mCherry (mCherry-LBR$^{1–533}$) or $(His)_6$ [$(His)_6$-LBR$^{1–533}$]. Localization of endogenous and exogenous Pom121 and RanGAP1 in cells in which the INM and ONM had been separated was examined by direct observation of its fluorescence or immunofluorescence staining 14 h posttransfection.

Antibodies

The following primary antibodies were used in immunofluorescence staining: mAb414 (MMS-120P; Covance, Princeton, NJ), diluted 1:3000; anti-GFP (598; MBL, Nagoya, Japan) and anti-RanGAP1 (33–0800; Zymed Laboratories, South San Francisco, CA) antibodies, diluted 1:1000; and rat antiserum raised against Pom121 (Funakoshi *et al.*, 2007), diluted 1:1000. Goat Alexa Fluor 488-, 594-, and 647-conjugated secondary antibodies and donkey Alexa Fluor 594- and 647-conjugated secondary antibodies (Invitrogen) were used at a dilution of 1:1000.

The following primary antibodies were used in Western blotting: anti-ELYS (BMR00513; Bio Matrix Research, Tokyo, Japan), anti-LBR (E398; Epitomics, Burlingame, CA), anti-Nup153 (QE5, ab24700; Abcam, Cambridge, MA), anti-Nup107 (A301–787A; Bethyl Laboratories, Montgomery, TX), anti-Nup53 (A301–781A; Bethyl), anti–importin β (sc-1136; Santa Cruz Biotechnology, Santa Cruz, CA), and anti-lamin B (sc-6217; Santa Cruz), all diluted 1:1000, and anti–importin α (610485; BD Transduction, Franklin Lakes, NJ), diluted 1:3000. To detect proteins, an enhanced chemiluminescence (ECL) detection kit (RPN2106; GE Healthcare, Piscataway, NJ) and the following horseradish peroxidase–conjugated antibodies were used: rabbit anti–rat immunoglobulin (Ig)G (A5795; Sigma, St. Louis, MO), goat anti–rabbit IgG (170–6515; Bio-Rad, Hercules, CA), goat anti–mouse IgG (170–6516; Bio-Rad), and rabbit anti–goat IgG (305–035-003; Jackson ImmunoResearch, West Grove, PA), all at a dilution of 1:3000.

Plasmid construction

pEXPR-P*EF-1*α-POM121$^{1–1249}$-Venus and pEXPR-P*EF-1*α-POM121$^{266–1249}$-Venus were generated as described previously (Funakoshi *et al.*, 2007). To generate constructs for the expression of Pom121 deletion and NLS mutants (Pom121$^{1–1249}$NLSmut,

Pom121$^{266–1249}$NLSmut, Pom121$^{1–1249(\Delta137–265)}$, and Pom121$^{1–1249(\Delta1–136)}$), site-directed mutagenesis was performed using specific primer pairs with the above-mentioned plasmids as templates. Pom121 fragments were expressed as C-terminal EGFP fusions. To generate constructs for the expression of Pom121 fragments (Pom121$^{1–494}$, Pom121$^{1–494}$NLSmut, Pom121$^{1–494(\Delta137–265)}$, Pom121$^{1–265}$, Pom121$^{1–137}$, and Pom121$^{137–265}$), coding fragments were amplified by PCR from the above-mentioned plasmids and subcloned into pEGFP-N vectors (Clontech). To generate a construct for the expression of Pom121$^{137–494}$, the *Sal* I-*Eco*RI fragment of pEXPR-P*EF-1*α-POM121$^{1–1249}$-Venus was subcloned into pEGFP-N3 (Clontech, Mountain View, CA). An SV40 T-antigen NLS sequence (GGPPKKKPKVEDP) was introduced into the C terminus of Pom121$^{1–265}$ and Pom121$^{1–494}$NLSmut using a pair of oligo DNAs carrying the above NLS coding sequence.

To generate recombinant Pom121 fragments (Pom121$^{137–513}$, Pom121$^{137–513}$NLSmut, Pom121$^{266–513}$, and Pom121$^{266–513}$NLSmut) as N-terminal GST fusions, each Pom121 coding region was amplified by PCR and subcloned into pGEX-6P-3 (GE Healthcare).

To obtain LBR cDNA, first-strand cDNA was synthesized from total RNA prepared from HeLa S3 cells using SuperScript III reverse transcriptase (18080–044; Invitrogen) and an oligo(dT)$_{20}$ primer. LBR cDNA was amplified from the first-strand cDNA. Sequences encoding amino acids 1–533 of LBR were amplified by PCR and introduced into pcDNA3.1/His (Invitrogen) and an expression vector that was generated by replacing the EGFP sequences of pEGFP-C1 with mCherry.

Cell fusion for visualization of interphase NPC assembly

Cells were synchronized at G_1/S by double-thymidine block [2 mM thymidine (T1895; Sigma), 16 h]. Pom121 knockdown was achieved through transfection of acceptor cells (stably expressing SECFP-H2B) with an siRNA oligonucleotide targeted to Pom121 using Lipofectamine 2000 (11668–019; Invitrogen) between the two thymidine block treatments. The oligonucleotide siRNA duplex used in this study was previously shown to be effective (oligo-2 in Funakoshi *et al*., 2007). As a control for Pom121 knockdown, cells were treated with transfection reagents alone. Cells were incubated with nocodazole (100 ng/ml in growth medium) (M1404; Sigma) for 3 h and then 8 h after the second thymidine block. Cell fusion was achieved as described previously (Maeshima *et al*., 2010). Briefly, mitotic cells were collected by shaking. Equal numbers of synchronized donor and acceptor cells were mixed and seeded onto poly-L-lysine–coated coverslips. After the completion of cytokinesis (~3 h after mitotic cell shake-off), cells were fused by incubation for 2 min in 50% PEG 1500 (10783641001; Roche, Basel, Switzerland]). After fusion, cells were incubated with aphidicolin (5 μg/ml in growth medium) (A0781; Sigma) for 16–17 h and fixed with 3.7% formaldehyde in phosphate-buffered saline (PBS). After immunostaining with Pom121 antiserum, middle-section images of heterokaryons with donor (higher intensity of Venus-Nup107) and acceptor (higher intensity of SECFP-H2B) nuclei were captured with a DeltaVisionRT microscope (Applied Precision, Issaquah, WA) using a Plan Apo 60×/1.40 oil-immersion objective (Olympus, Center Valley, PA). All images are presented without deconvolution. In heterokaryons, the fluorescence intensities of the Venus-Nup107 and Pom121 signals at the nuclear rim were measured using SoftWorx software (Applied Precision).

Immunofluorescence staining

Cell fixation and staining were performed as described previously (Maeshima *et al*., 2006), with minor modifications. Cells grown on coverslips were washed and fixed through incubation with freshly prepared 2% paraformaldehyde in PBS for 15 min. In case of heterokaryons, cells were fixed through incubation with 3.7% formaldehyde in PBS for 10 min. Fixed cells were treated with 50 mM glycine in PBS for 5 min, permeabilized with 0.5% Triton X-100 in PBS for 5 min, and blocked through incubation with 5% normal goat serum (NGS; Chemicon, Temecula, CA) in PBS for 1 h. They were then incubated with the primary antibody in PBS containing 1% NGS for 2 h. After washing, cells were next incubated with secondary antibody in PBS containing 1% NGS for 1 h. After washing, coverslips were mounted in PPDI [80% glycerol, 1 mg/ml paraphenylenediamine (164–01532; Wako, Richmond, VA)] in PBS. In some cases, cells were stained with 4′,6-diamidino-2-phenylindole (DAPI; 1 μg/ml; Roche) before mounting. When primary goat antibodies were used, 3% skim milk in PBS was used as the blocking solution, with donkey antibodies as secondary antibodies. Image stacks (0.2-μm sections) were recorded with a DeltaVisionRT microscope (Applied Precision) using PlanApo 60×/1.40 and UPlanApo 100×/1.35 oil-immersion objectives (Olympus). All the images are presented without deconvolution.

Pull-down assay

Human Pom121 fragments and NLS mutants comprising amino acids 137–513 and 266–513 tagged with GST at their N termini were expressed from a pGEX6p-3 vector in *Escherichia coli* BL21 and purified with Glutathione Sepharose 4B beads (17–0756; GE Healthcare). Because the GST-Pom121$^{137–513}$ peptide became unstable during purification, a (His)$_6$ tag was added to its C terminus, and it was isolated using Ni-NTA agarose (30210; Qiagen) prior to purification with Glutathione Sepharose 4B. GST-Pom121 peptide–coated beads and GST-coated beads were incubated for 1 h with cytosol from HeLa cells, which was prepared based on the report by Hawryluk-Gara *et al*. (2005). Briefly, cells were suspended in lysis buffer (20 mM Tris-HCl [pH 7.5], 400 mM NaCl, 1 mM EDTA, 1% Triton X-100, 0.1% Tween 20, 1 mM phenylmethylsulfonyl fluoride, protease inhibitor cocktail [11873580001; Roche]), sonicated, and centrifuged at 15,000 *g* for 30 min at 4°C. Supernatants were diluted 3.75-fold in binding buffer, giving final concentrations of Triton X-100 and NaCl of 0.3% and 106 mM, respectively, and centrifuged at 15,000 *g* for 15 min at 4°C. GST-Pom121 fragments and GST-coated beads were incubated with the diluted supernatants, washed with binding buffer, eluted in sample buffer, and analyzed by Western blotting.

To observe direct interactions, wild-type and NLS mutant GST-Pom121$^{266–513}$–coated Glutathione Sepharose 4B beads were incubated for 1 h at 4°C with recombinant importin α, importin β, or transportin. These proteins had all been purified as previously reported (Imamoto *et al*., 1995), and their concentrations had been adjusted to 0.8 μM in TB buffer (20 mM HEPES [pH 7.3], 110 mM potassium acetate, 2 mM magnesium acetate, 5 mM sodium acetate, 0.5 mM EGTA, 1 mM dithiothreitol, protease inhibitor cocktail [11873580001; Roche]). After washing with TB buffer, proteins were eluted in sample buffer and analyzed by Western blotting with anti–importin α and anti–importin β antibodies.

FRAP analysis

HeLa cells growing on glass-bottom dishes were transfected with the plasmids described earlier in text (see "Cells and transfection"). After incubation for 17 h at a permissive temperature (32°C), FRAP analysis was performed using a quantifiable laser module (50 mW, 488-nm solid-stable laser) and a DeltaVision RT restoration microscope system (Olympus), the latter equipped with a PlanApo 60×/1.40 oil-immersion objective (Olympus). The laser was focused

to a spot on the NE, and bleaching was performed with a single 200-ms stationary pulse at 50% laser power. The first image was acquired ~20 ms after bleaching. Subsequent images were captured every 5 min until 60 min postbleaching. The fluorescence intensity of each spot was measured using SoftWorx software (Applied Precision). The mean intensity values at time t of a bleached NE surface spot (a_t), a nonbleached NE surface spot (b_t), and an area outside the cell (background, c_t) were determined, and relative fluorescence recovery was calculated as $(a_t - c_t) / (b_t - c_t)$. Each portion of the calculated value at $t = 0$ was plotted.

ACKNOWLEDGMENTS

We thank A. Miyawaki, T. Nagai, and R. Tsien for their gifts of Venus and SECFP. We also thank members of the Cellular Dynamics Lab for their helpful comments. We are grateful to R. Nakazawa, Y. Ichikawa, and the Support Unit at the RIKEN BSI Research Resources Center for help with DNA sequencing. This work was supported by a MEXT grant-in-aid and from RIKEN Special Project Funding for Basic Science (Bioarchitect Project and Cellular System Project).

REFERENCES

Alber F *et al.* (2007). The molecular architecture of the nuclear pore complex. Nature 450, 695–701.

Antonin W, Franz C, Haselmann U, Antony C, Mattaj IW (2005). The integral membrane nucleoporin pom121 functionally links nuclear pore complex assembly and nuclear envelope formation. Mol Cell 17, 83–92.

Cronshaw JM, Krutchinsky AN, Zhang W, Chait BT, Matunis MJ (2002). Proteomic analysis of the mammalian nuclear pore complex. J Cell Biol 158, 915–927.

D'Angelo MA, Anderson DJ, Richard E, Hetzer MW (2006). Nuclear pores form de novo from both sides of the nuclear envelope. Science 312, 440–443.

Daigle N, Beaudouin J, Hartnell L, Imreh G, Hallberg E, Lippincott-Schwartz J, Ellenberg J (2001). Nuclear pore complexes form immobile networks and have a very low turnover in live mammalian cells. J Cell Biol 154, 71–84.

Doucet CM, Talamas JA, Hetzer MW (2010). Cell cycle-dependent differences in nuclear pore complex assembly in metazoa. Cell 141, 1030–1041.

Dultz E, Zanin E, Wurzenberger C, Braun M, Rabut G, Sironi L, Ellenberg J (2008). Systematic kinetic analysis of mitotic dis- and reassembly of the nuclear pore in living cells. J Cell Biol 180, 857–865.

Fichtman B, Ramis C, Rasala B, Harel A, Forbes DJ (2010). Inner/outer nuclear membrane fusion in nuclear pore assembly: biochemical demonstration and molecular analysis. Mol Biol Cell 21, 4197–4211.

Flemming D, Sarges P, Stelter P, Hellwig A, Bottcher B, Hurt E (2009). Two structurally distinct domains of the nucleoporin Nup170 cooperate to tether a subset of nucleoporins to nuclear pores. J Cell Biol 185, 387–395.

Funakoshi T, Maeshima K, Yahata K, Sugano S, Imamoto F, Imamoto N (2007). Two distinct human POM121 genes: requirement for the formation of nuclear pore complexes. FEBS Lett 581, 4910–4916.

Frey S, Görlich D (2007). A saturated FG-repeat hydrogel can reproduce the permeability properties of nuclear pore complexes. Cell 130, 512–523.

Hallberg E, Wozniak RW, Blobel G (1993). An integral membrane protein of the pore membrane domain of the nuclear envelope contains a nucleoporin-like region. J Cell Biol 122, 513–521.

Harel A, Chan RC, Lachish-Zalait A, Zimmerman E, Elbaum M, Forbes DJ (2003a). Importin beta negatively regulates nuclear membrane fusion and nuclear pore complex assembly. Mol Biol Cell 14, 4387–4396.

Hawryluk-Gara LA, Shibuya EK, Wozniak RW (2005). Vertebrate Nup53 interacts with the nuclear lamina and is required for the assembly of a Nup93-containing complex. Mol Biol Cell 16, 2382–2394.

Hetzer M, Gruss OJ, Mattaj IW (2002). The Ran GTPase as a marker of chromosome position in spindle formation and nuclear envelope assembly. Nat Cell Biol 4, E177–184.

Iino H, Maeshima K, Nakatomi R, Kose S, Hashikawa T, Tachibana T, Imamoto N (2010). Live imaging system for visualizing nuclear pore complex (NPC) formation during interphase in mammalian cells. Genes Cells 15, 647–660.

Imamoto N, Shimamoto T, Kose S, Takao T, Tachibana T, Matsubae M, Sekimoto T, Shimonishi Y, Yoneda Y (1995). The nuclear pore-targeting complex binds to nuclear pores after association with a karyophile. FEBS Lett 368, 415–419.

Lusk CP, Blobel G, King MC (2007). Highway to the inner nuclear membrane: rules for the road. Nat Rev Mol Cell Biol 8, 414–420.

Maeshima K *et al.* (2010). Nuclear pore formation but not nuclear growth is governed by cyclin-dependent kinases (CDKS) during interphase. Nat Struct Mol Biol 17, 1065–1072.

Maeshima K, Yahata K, Sasaki Y, Nakatomi R, Tachibana T, Hashikawa T, Imamoto F, Imamoto N (2006). Cell-cycle-dependent dynamics of nuclear pores: pore-free islands and lamins. J Cell Sci 119, 4442–4451.

Makio T, Stanton LH, Lin CC, Goldfarb DS, Weis K, Wozniak RW (2009). The nucleoporins Nup170p and Nup157p are essential for nuclear pore complex assembly. J Cell Biol 185, 459–473.

Mansfeld J *et al.* (2006). The conserved transmembrane nucleoporin NDC1 is required for nuclear pore complex assembly in vertebrate cells. Mol Cell 22, 93–103.

Maul GG, Price JW, Lieberman MW (1971). Formation and distribution of nuclear pore complexes in interphase. J Cell Biol 51, 405–418.

Nishimoto T, Eilen E, Basilico C (1978). Premature chromosome condensation in a ts DNA-mutant of BHK cells. Cell 15, 475–485.

Nishitani H, Ohtsubo M, Yamashita K, Iida H, Pines J, Yasudo H, Shibata Y, Hunter T, Nishimoto T (1991). Loss of RCC1, a nuclear DNA-binding protein, uncouples the completion of DNA replication from the activation of cdc2 protein kinase and mitosis. EMBO J 10, 1555–1564.

Onischenko E, Stanton LH, Madrid AS, Kieselbach T, Weis K (2009). Role of the Ndc1 interaction network in yeast nuclear pore complex assembly and maintenance. J Cell Biol 185, 475–491.

Rabut G, Doye V, Ellenberg J (2004a). Mapping the dynamic organization of the nuclear pore complex inside single living cells. Nat Cell Biol 6, 1114–1121.

Rabut G, Lenart P, Ellenberg J (2004b). Dynamics of nuclear pore complex organization through the cell cycle. Curr Opin Cell Biol 16, 314–321.

Rasala BA, Ramos C, Harel A, Forbes DJ (2008). Capture of AT-rich chromatin by ELYS recruits POM121 and NDC1 to initiate nuclear pore assembly. Mol Biol Cell 19, 3982–3996.

Rexach M (2009). Piecing together nuclear pore complex assembly during interphase. J Cell Biol. 185, 377–379.

Rout MP, Aitchison JD (2000). Pore relations: nuclear pore complexes and nucleocytoplasmic exchange. Essays Biochem 36, 75–88.

Ryan KJ, McCaffery JM, Wente SR (2003). The Ran GTPase cycle is required for yeast nuclear pore complex assembly. J Cell Biol 160, 1041–1053.

Stavru F, Nautrup-Pedersen G, Cordes VC, Görlich D (2006). Nuclear pore complex assembly and maintenance in POM121- and gp210-deficient cells. J Cell Biol 173, 477–483.

Söderqvist H, Imreh G, Kihlmark M, Linnman C, Ringertz N, Hallberg E (1997). Intracellular distribution of an integral nuclear pore membrane protein fused to green fluorescent protein—localization of a targeting domain. Eur J Biochem 250, 808–813.

Tahara K *et al.* (2008). Importin-beta and the small guanosine triphosphatase Ran mediate chromosome loading of the human chromokinesin Kid. J Cell Biol 180, 493–506.

Vasu SK, Forbes DJ (2001). Nuclear pores and nuclear assembly. Curr Opin Cell Biol 13, 363–375.

Wilson KL, Berk JM (2010). The nuclear envelope at a glance. J Cell Sci 123, 1973–1978.

Yavuz S, Santarella-Mellwig R, Koch B, Jaedicke A, Mattaj IW, Antonin W (2010). NLS-mediated NPC functions of the nucleoporin Pom121. FEBS Lett 584, 3292–3298.

Zwerger M, Kolb T, Richter K, Karakesisoglou I, Herrmann H (2010). Induction of a massive endoplasmic reticulum and perinuclear space expansion by expression of lamin B receptor mutants and the related sterol reductases TM7SF2 and DHCR7. Mol Biol Cell 21, 354–368.